厚生労働科学研究費補助金（痴呆・骨折臨床研究事業）
分担研究報告書

痴呆性疾患の介入予防に関する研究
（睡眠からの介入研究の理論指導と実践に関する研究）

分担研究者　白川 修一郎　国立精神・神経センター精神保健研究所　室長

研究要旨：高齢者では、睡眠障害が認知機能低下の引き起こし、痴呆性疾患発症の予防に睡眠健康改善が有用であり、睡眠に係わる生活習慣のセルフマネージメント方式による改善で、睡眠健康が短期間で増進する。睡眠改善に係わる生活習慣のセルフマネージメントのなかの夕方の軽運動の覚醒水準増進へのメカニズムについて検討した。

A. 研究目的

高齢者の痴呆性疾患の予防介入を、睡眠改善の面から遂行するための実践技術の開発及び確立とその科学的基盤解明を目的とする。

B. 研究方法

1. 睡眠のセルフマネージメント改善技術のうち、基礎的背景が不明瞭な夕方の短時間軽運動による薄明期の覚醒水準上昇効果の基礎的研究を行い、そのメカニズムの解明を試みた。被験者は運動習慣を有する健常男性12人（22～27歳）であり、事前に実験内容を十分に説明して書面による実験参加の同意を得た。被験者は通常の就床時刻の10時間30分後（CT10:30）から、間に20分間の休憩を挟む25分間のペダリング運動（最大酸素摂取量の60%強度）を2回（計50分）実施した。他の実験条件として、運動を行わずに安静状態を続ける対照条件、および前夜の睡眠時間を90分短縮して同様の運動を行う部分断眠＋運動条件の計３条件を設け、実験順序を被験者毎にランダムに設定した。測定項目は、直腸温の連続測定、および主観的気分と眠気、安静覚醒閉眼脳波、事象関連電位（P300）、および計算課題と作業記憶課題とし、これらについては運動前、1回目の運動終了後、2回目の運動終了直後、30分、1、2、3、4、5時間後に測定した。
2. 運動習慣と睡眠との関係を検討するため、首都圏在住のスポーツクラブに所属し運動習慣を持つ40代～60代の283名の中高年女性と運動習慣をまったく持たないランダムにサンプリングされた40代～60代の567名の中高年女性について秋季と春期に睡眠健康および運動習慣についての調査を行った。なお、対象者は事前に調査内容を十分に説明して書面による参加の同意の得られたものである。睡眠習慣と睡眠健康調査票は、高齢者の睡眠のセルフマネージメント改善評価に用いたものを使用した。

（倫理面への配慮）
研究内容を書面で十分に説明し、自由意志で

の参加で、書面にて同意の得られた者のみを対象者とした。

C. 研究結果

1. 運動による直腸温上昇は平均約 0.8℃であったが、部分断眠＋運動条件では、それよりも 0.3℃高い平均約 1.1℃の上昇が認められた。この上昇した直腸温が対照条件の水準まで低下するのには、両運動条件とも約 2 時間半を要した。visual analogue scale で評価した集中力、および KSS で評価した主観的眠気は、部分断眠＋運動条件の運動 1 時間後に集中力低下と眠気の亢進を示した。これらと同期して計算課題の成績低下が認められ、回答数、正解率、回答時間の変動係数のいずれも全測定中で最低値を示した。また対照条件では CT14:40 において主観的眠気の亢進が認められたが、運動および部分断眠＋運動条件では、それよりも早い CT12:10 および CT12:40（運動終了 30 分後および 1 時間後）において主観的眠気の亢進が認められた。P300 では、潜時が全ての実験条件で運動前（CT10:00）および運動 5 時間後（CT16:40）に最短となり、その間の時間帯で延長していたが、部分断眠＋運動条件の運動 2 時間後の値が最も延長していた。また P300 のオッドボール課題に対する反応時間は、部分断眠＋運動条件の運動 30 分後において最も遅延した。

2. 加齢による影響を排除した解析結果では、就床・起床時刻と睡眠時間には運動習慣の有無による影響は認められなかった。しかし、就床・起床時刻と睡眠時間の規則性は、運動群において有意に規則性が高かった。睡眠健康では、睡眠維持の因子得点が運動群において良好であり、入眠困難性は 40 代、50 代の非運動群において有意に悪化していた。

D. 考察

睡眠のセルフマネージメント改善技術のうち、夕方の短時間軽運動が有意に夜間睡眠を改善する事実が得られているが、その科学的基盤が不明瞭であった。これまでも運動と睡眠健康との間には密接な関係のあるとの報告は多いが、運動強度や運動負荷時間によっては夜間睡眠を障害するとの報告も散見される。

中高年、老年女性を対象とした本研究者らの調査では、40 代、50 代では運動習慣は円滑な入眠を促進していることが判明した。また、調査対象の全年齢層において睡眠維持を改善させているとの結果であった。一方で、これらの改善効果は、運動習慣を有する者が睡眠習慣の高い規則性を有することによる二次的な影響である可能性も排除できないものであった。

高齢者の睡眠障害を想定し 90 分の部分断眠を行った後の運動負荷では、深部体温の上昇が非断眠群と比べてより大きく上昇する結果であった。深部体温の上昇は認知機能、作業能力の上昇を引き起こし、覚醒水準を上昇させることも判明した。一方で、運動負荷後の眠気の上昇と脳機能の低下は、部分断眠群において最も早く発現することが明らかとなった。これらの結果は、運動前夜の睡眠の状態とも併せて覚醒水準および認知機能の日内変動に運動が何らかの影響を与えることを示唆するものである。

E. 結論

習慣的な軽運動は、睡眠維持と入眠の改善に有効であることが判明した。特に、睡眠が不足した状態での軽運動負荷は、深部体温、覚醒水準、認知機能の上昇をより引き起こしやすく、その後の反跳的低下をもたらしやすいことが基礎的実験により明らかとなった。高齢者における夕方の軽運動習慣の睡眠改

善効果は、運動時の深部体温上昇、認知機能上昇によりその後の反跳的体温低下と覚醒水準の低下を促進し、円滑な入眠を引き起こし睡眠を安定維持させていることが明確となった。

F. 研究発表

1. 論文発表

a. Tanaka H, Shirakawa S: Sleep health, lifestyle and mental health in the Japanese eilderly ensuring sleep to promote a healthy brain and mind. J Psychosomatic Research 56: 465-477, 2004.

b. 水野康，国井実，清田隆毅，小野茂之，駒田陽子，白川修一郎：中高年女性における運動習慣の有無と睡眠習慣および睡眠健康度との関係．体力医学 53(5): 527-536, 2004.

c. 小野茂之，駒田陽子，有賀元，塘久夫，白川修一郎：首都圏の女性を対象とした睡眠健康と便通状態の関係についての調査．日本生理人類学会誌 9(1): 15-21, 2004.

2. 学会発表

a. 水野康，駒田陽子，小野茂之，白川修一郎：中高年女性における運動習慣と睡眠習慣・睡眠健康に関する横断的調査研究．日本睡眠学会第 29 回定期学術集会，東京，2004.7.1-2.

b. 水野康，駒田陽子，北堂真子，白川修一郎：運動後における覚醒水準および認知機能の経時的変化．日本睡眠学会第 29 回定期学術集会，東京，2004.7.1-2.

c. 駒田陽子，水野康，朝田隆，片野綱大，松岡恵子，白川修一郎：高齢者に対するセルフマネージメント方式睡眠改善介入効果．日本睡眠学会第 29 回定期学術集会，東京，2004.7.1-2.

d. 小野茂之，駒田陽子，有賀元，塘久夫，白川修一郎：睡眠健康に対する便通状態の影響－首都圏成人女性の実態調査より．日本睡眠学会第 29 回定期学術集会，東京，2004.7.1-2.

e. 駒田陽子，白川修一郎：セルフマネージメント方式による睡眠改善介入技術の高齢者における検討，日本心理学会第 68 回大会，大阪，2004.9.12-14.

f. 水野康，白川修一郎：運動および部分断眠後の運動がその後の覚醒水準および認知機能に及ぼす影響，第 59 回日本体力医学会，埼玉，2004.9.14-16.

g. Komada Y, Adachi N, Mizuno K, Aritomi R, Shirakawa S: The influence of sleep health and sleep habits of parents on those of children in Japan. 17th Congress of the European Sleep Research Society, Prague, Czech Republic, October 5-9, 2004.

G. 知的所有権の取得状況

1. 特許取得

なし

2. 実用新案登録

なし

3. その他

なし

Ⅲ.　研究成果の刊行に関する一覧表

別紙４

研究成果の刊行に関する一覧表

雑誌

発表者氏名	論文タイトル名	発表誌名	巻　号	ページ	出版年
Cichocki A, Shishkin SL, Musha T, Leonowicz Z, Asada T, Kurachi T.	EEG fitering based on blind source separation (BSS) for early detection of Alzheimer' s disease.	Clin Neurophysiol	116	729-737	2005
Zhi-Jie L, Matsuda H, Asada T, Ohnishi T, Kanetaka H, Imabayashi E, Tanaka F.	Gender difference in brain perfusion 99m-ECD SPECT in aged healthy volunteers after correction for partial volume effects.	Nucl Med Commun	25	999-1005	2004
Imabayashi E, Matsuda H, Asada T, Ohnishi T, Sakamoto S, Nakano S, Inoue T.	Superiority of 3-dimensional stereotactic surface projection analysis over visual inspection in discrimination of patients with very early Alzheimer' s disease from controls using brain perfusion SPECT.	J Nucl Med	45	1450-1457	2004

発表者氏名	論文タイトル名	発表誌名	巻　号	ページ	出版年
Kanetaka H, Matsuda H, Asada T, Ohnishi T, Yamashita F, Tanaka F, Nakano S, TakasakiY.	Effects of partial volume correction on discrimination between very early Alzheimer's dementia and controls using brain perfusion SPECT.	Eur J Nucl Med Mol Imaging.	31	975-980	2004
根本清貴、山下典生、大西隆、今林悦子、平尾健太郎、横銭拓、佐々木恵美、水上勝義、松田博史、朝田隆	軽度認知機能障害の脳血流および形態変化－茨城県利根町における横断研究－	Dementia Japan	18	263-273	2004
Y Tashima, R Oe, S Lee, G Sugihara, E.J.Chambers, M Takahashi, T Yamada	The effect of cholesterol and monosialoganglioside (GM1) on the release and aggregation of Amyloid beta-peptide frome liposomes prepared from brain membrane-like lipids	J Biol Chem	279(17)	17587-17595	2004
Y Matsunaga, A Fujii, A Awasthi, J Yokotani, T Takakura, T Yamada	Eight-residue Aβ peptides inhibit the aggregation and enzymatic activity of Aβ42	Regulatory Peptides	120	227-236	2004
鉾石和彦，小森憲治郎，田辺敬貴	アルツハイマー病 - 神経心理学 -	カレントテラピー	22	341-346	2004

発表者氏名	論文タイトル名	発表誌名	巻　号	ページ	出版年
Tanaka H, Shirakawa S	Sleep health, lifestyle and mental health in the Japanese eilderly ensuring sleep to promote a healthy brain and mind.	J Psychosomatic Research	56	465-477	2004

Ⅳ. 研究成果の刊行物・別刷

ELSEVIER

Clinical Neurophysiology 116 (2005) 729–737

www.elsevier.com/locate/clinph

EEG filtering based on blind source separation (BSS) for early detection of Alzheimer's disease

Andrzej Cichocki[a,b,*], Sergei L. Shishkin[a], Toshimitsu Musha[c], Zbigniew Leonowicz[a,d], Takashi Asada[e], Takayoshi Kurachi[c]

[a]*Laboratory for Advanced Brain Signal Processing, RIKEN Brain Science Institute, 2-1 Hirosawa, Wako-shi, Saitama 351-0198, Japan*
[b]*Warsaw University of Technology, Warsaw, Poland*
[c]*Brain Functions Laboratory Inc., KSP Building E211, Sakado, Takatsu Kawasaki, Kanagawa, 213-0012, Japan*
[d]*Wroclaw University of Technology, Wroclaw, Poland*
[e]*Department of Neuropsychiatry, Tsukuba University, Tennoudai, Tsukuba-shi, 305-8575, Japan*

Accepted 16 September 2004
Available online 28 October 2004

Abstract

Objective: Development of an EEG preprocessing technique for improvement of detection of Alzheimer's disease (AD). The technique is based on filtering of EEG data using blind source separation (BSS) and projection of components which are possibly sensitive to cortical neuronal impairment found in early stages of AD.

Methods: Artifact-free 20 s intervals of raw resting EEG recordings from 22 patients with Mild Cognitive Impairment (MCI) who later proceeded to AD and 38 age-matched normal controls were decomposed into spatio-temporally decorrelated components using BSS algorithm 'AMUSE'. Filtered EEG was obtained by back projection of components with the highest linear predictability. Relative power of filtered data in delta, theta, alpha 1, alpha 2, beta 1, and beta 2 bands were processed with Linear Discriminant Analysis (LDA).

Results: Preprocessing improved the percentage of correctly classified patients and controls computed with jack-knifing cross-validation from 59 to 73% and from 76 to 84%, correspondingly.

Conclusions: The proposed approach can significantly improve the sensitivity and specificity of EEG based diagnosis.

Significance: Filtering based on BSS can improve the performance of the existing EEG approaches to early diagnosis of Alzheimer's disease. It may also have potential for improvement of EEG classification in other clinical areas or fundamental research. The developed method is quite general and flexible, allowing for various extensions and improvements.

Keywords: Alzheimer's disease; Diagnosis; EEG; Blind Source Separation; AMUSE; Filtering

1. Introduction

Alzheimer's disease (AD) is one of the most frequent disorders among the elderly population (Jeong, 2004; Petersen, 2003). Recent studies have demonstrated that AD has a presymptomatic phase, likely lasting years, during which neuronal degeneration is occurring but clinical symptoms do not yet appear. This makes preclinical discrimination between people who will and will not ultimately develop AD critical for early treatment of the disease which could prevent or at least slow down the onset of clinical manifestations of disease (Blennow and Hampel, 2003; DeKosky and Marek, 2003; Rapoport, 2000; Wagner, 2000). Moreover, early diagnostic tools could significantly facilitate the development of drugs for the treatment at the early stage of AD: without preclinical diagnosis, many times more subjects (potential patients with huge percentage of those who actually would never develop AD) should be involved for testing of these drugs (DeKosky and Marek, 2003). A diagnostic method should be relatively inexpensive to make possible screening of many individuals who are at risk of developing this dangerous disease

* Corresponding author. Tel.: +81 48 467 9668; fax: +81 48 467 9686.
E-mail address: cia@brain.riken.jp (A. Cichocki).

1388-2457/$30.00 © 2004 Published by Elsevier Ireland Ltd. on behalf of International Federation of Clinical Neurophysiology.
doi:10.1016/j.clinph.2004.09.017

(DeKosky and Marek, 2003). The electroencephalogram (EEG) is one of the most promising candidates to become such a method.

To date, many signal processing techniques were applied for revealing pathological changes in EEG associated with AD (see Jeong, 2004, for review). For example, combination of linear and nonlinear measures improved the classification accuracy of AD versus normal subjects up to 92% (Pritchard et al., 1994). Using principal component analysis (PCA) as a postprocessing tool for compressing linear and nonlinear EEG features over channels and age as a moderator variable in a study with rigorous validation procedure (jack-knifing), Besthorn et al. (1997) obtained 89% correct classification. However, high classification accuracy was obtained for patients who already developed serious cognitive impairment (e.g. Mini Mental State Examination (MMSE) score was 11.5 ± 7.9 in the study of Besthorn et al. (1997)).

Finding a method for identification of patients who have no clinical signs of AD at the moment of EEG registration but later progress to AD is the main challenge in this field. The studies of this kind are very rare. Huang et al. (2000) obtained 87% classification accuracy for discrimination between patients with mild cognitive impairment (MCI) who later progressed and not progressed to AD, however, without reporting the use of cross-validation. Musha and co-authors demonstrated, in a computer simulation, that local cortical neuronal impairment should lead to lower dipolarity (goodness-of-fit for dipole localizations) of alpha EEG frequency components (Hara et al., 1999), and then, based on these results, developed a technique for estimation of cortical impairment in AD using a single index of dipolarity (Musha et al., 2002). Alpha dipolarity was able to differentiate MCI patients who showed no clinical signs of AD at the time when EEG was recorded but developed AD later, as diagnosed in the follow-up, from normal controls with high probability; it also correlated with the degree of cortical neuronal impairment, estimated by SPECT (Musha et al., 2002).

However, in spite of all of the achievements made in the above cited studies, the problem of preclinical diagnosis of AD using EEG is not yet solved and further improvement of the methodology is necessary.

The main idea of this paper can be formulated as 'filtering based on Blind Source Separation (BSS)', that is, filtering of EEG by selection of most relevant components followed by reconstruction of the relevant part (subspace) of EEG signal using back projection of only these components. We propose a preprocessing technique based on this idea for improving EEG-based AD diagnosis (possibly useful also in other fields of EEG analysis). Its usefulness was evaluated in combination with standard procedures, namely the linear discriminant analysis (LDA) applied to spectral power in several frequency bands. To make comparison clear and fair, we used only most reliable but simple procedures. However, more sophisticated analysis based on recent advances in techniques for EEG processing and data classification may provide, in combination with proposed preprocessing, further significant improvement of early AD diagnosis, and some relevant emerging techniques will be mentioned in Discussion.

2. Methods

2.1. Blind source separation filtering for EEG classification

Intuitively, one can expect that some hidden components of such a complex signal like EEG can be more sensitive to Alzheimer's disease and the related disorders than others. These more sensitive components can be considered as useful 'signal', and the other components of EEG as 'noise' or 'unwanted signals'. Improving the 'signal-to-noise ratio' by filtering off the 'noise' could enhance the performance of subsequent feature extraction and data classification. Blind Source Separation (BSS) algorithms (see Cichocki and Amari, 2003, for extensive review) can be used for the purpose of such filtering.

BSS, in its application to EEG analysis, assume that EEG signal is composed of a finite number of components (signals from the brain and other sources), $s(t) = [s_1(t),\ldots,s_n(t)]^T$. Here t is a discrete time index, n is the number of components and $[\ldots]^T$ means transpose of row vector. Components are mixed through unknown linear mixing process (described by $n \times n$ mixing matrix $\mathbf{A}$), and n sensors (EEG electrodes) record the mixed signals $\mathbf{x}(t) = \mathbf{A}\mathbf{s}(t)$. Each of the components changes in time, but has a fixed weight for each channel. BSS algorithm finds an unmixing (separating) $n \times n$ matrix $\mathbf{W}$ consisting of coefficients with which the electrode signals should be taken to form, by summation, the estimated components: $\mathbf{y}(t) = \mathbf{W}\mathbf{x}(t)$. (In more general case, the number of components can be not equal to the number of sensors.) The entries of the estimated mixing matrix $\hat{\mathbf{A}} = \mathbf{W}^{-1}$ are components' weights in the mixing process; in other words, they indicate how strongly each electrode picks up each of individual components. *Back projection* of some selected components $\mathbf{x}_r(t) = \mathbf{W}^{-1}\mathbf{y}_r(t)$ (where $\mathbf{x}_r(t)$ is a vector of reconstructed sensor signals and $\mathbf{y}_r(t)$ is the vector obtained from the vector $\mathbf{y}(t)$ after removal of all the undesirable components (i.e. by replacing them with zeros)) allows us to filter the EEG data.

In strict sense, BSS means estimation of true (original) sources, though exactly the same procedure can be used for separation of two or more subspaces of the signal without estimation of true sources. One procedure currently becoming popular in EEG analysis is removing artifact-related BSS components and back projection of components originating from brain (e.g. Jung et al., 2000; Joyce et al., 2004; Vorobyov and Cichocki, 2002). In this procedure, components of brain origin are not required to be separated from each other exactly, because they are mixed again by

back projection after removing artifact-related components. But by the same procedure we can filter off the 'noise' also in wider sense, improving the relative amount of any types of useful information in the signal. Specifically, we can try to increase the relative amount of signal content related to AD (i.e. to improve signal to noise ratio — SNR).

Finding the rules or fundamental principles for identification of *relevant and irrelevant components* is critical for the proposed approach and, in general, may require extensive studies. In the case of removing artifact-related components, such components typically can be easily identified by visual inspection, but in more general case exact discrimination of relevant and non-relevant components is more difficult. In this paper we attempt to differentiate clusters or subspaces of components with similar properties or features. For the purposes of EEG classification the estimation of individual components corresponding to separate and meaningful brain sources is not required, unlike in other applications of BSS to EEG processing (including its most popular variant, Independent Component Analysis (ICA)). The use of clusters of components is especially beneficial when the data from different subjects are compared: similarity between individual components in different subjects is usually low, while subspaces formed by similar components are more likely to be sufficiently overlapped. Differentiation of subspaces with high and low amount of diagnostically useful information can be made easier if components are separated and sorted according to some criteria which, at least to some extent, correlate with the diagnostic value of components. BSS algorithm 'AMUSE', in our opinion, can be relevant for this task.

2.2. AMUSE algorithm and its properties

AMUSE (Cichocki and Amari, 2003; Szupiluk and Cichocki, 2001; Tong et al., 1991, 1993)) is a BSS algorithm which arranges components not only in the order of decreasing variance (that is typical for the use of singular value decomposition (SVD) which is implemented within the algorithm), but also in the order of their decreased linear predictability. Low values for both characteristics can be specific for many of EEG components related to high frequency artifacts, especially electromyographic signal (which cannot be sufficiently removed by usual filtering in frequency domain, see Goncharova et al., 2003). Thus, a first attempt of selection of diagnostically important components can be made by removing a range of components separated with AMUSE (below referred to as 'AMUSE components') with the lowest linear predictability. Automatic sorting of components by this algorithm makes it possible to do this simply by removing components with indices higher than some chosen value.

AMUSE algorithm belongs to the group of second-order-statistics spatio-temporal decorrelation (SOS-STD) BSS algorithms. It provides similar decomposition as the well known and popular SOBI algorithms (Belouchrani et al., 1997; Tang et al., 2002). AMUSE algorithm uses simple principles that the estimated components should be spatio-temporally decorrelated and be less complex (i.e. have better linear predictability) than any mixture of those sources. The components are ordered according to decreasing values of singular values of a time-delayed covariance matrix. As in Principal Component Analysis (PCA) and unlike in many ICA algorithms, all components estimated by AMUSE are uniquely defined (i.e. any run of algorithms on the same data will always produce the same components) and consistently ranked. Fig. 1 illustrates typical components obtained by decomposing EEG using AMUSE algorithm.

AMUSE algorithm can be considered as two consecutive PCAs: first, PCA is applied to input data; second, PCA (SVD) is applied to the time-delayed covariance matrix of the output of previous stage. In the first step standard or robust prewhitening (sphering) is applied as a linear transformation $\mathbf{z}(t)=\mathbf{Q}\mathbf{x}(t)$, where $\mathbf{Q}=\mathbf{R}_x^{-\frac{1}{2}}$ of the standard covariance matrix $\mathbf{R}_x=E\{\mathbf{x}(t)\mathbf{x}^T(t)\}$ and $\mathbf{x}(t)$ is a vector of observed data for time instant t. Next, SVD is applied to a time-delayed covariance matrix of pre-whitened data: $\mathbf{R}_z=E\{\mathbf{z}(t)\mathbf{z}^T(t-1)\}=\mathbf{U}\mathbf{S}\mathbf{V}^T$, where $\mathbf{S}$ is a diagonal matrix with decreasing singular values and $\mathbf{U}$, $\mathbf{V}$ are matrices of eigenvectors. Then, an unmixing matrix is estimated as $\mathbf{W}=\hat{\mathbf{A}}^{-1}=\mathbf{U}^T\mathbf{Q}$ or $\hat{\mathbf{A}}=\mathbf{Q}^T\mathbf{U}$.

AMUSE algorithm is much faster than the vast majority of BSS algorithms (its processing speed is mainly defined by the PCA processing within it) and is very easy to use, because no parameters are required. It is implemented as a part of package 'ICALAB for signal processing' (Cichocki et al., online) freely available online and can be called also from the current version of EEGLAB toolbox (Delorme and Makeig, 2004) (which is freely available online at http://www.sccn.ucsd.edu/eeglab/) if both toolboxes are installed.

2.3. Subjects and EEG recording

We used EEG recordings collected in the previous study (Musha et al., 2002). In that study, patients who complained only for memory impairment, but had no apparent loss in general cognitive, behavioral, or functional status, were recruited. Fifty-three patients of this group met the following criteria for Mild Cognitive Impairment (MCI): MMSE score 24 or higher, Clinical Dementia Rating (CDR) scale score of 0.5 with memory performance less than one standard deviation below the normal reference (Wechsler Logical Memory Scale and Paired Associates Learning subtests, IV and VII, ≤ 9 (Wechsler, 1987), and/or ≤ 5 on the 30 min delayed recall of the Rey-Osterreith figure test (Hodges, 1993)). These patients were followed clinically for 12–18 months. Twenty-five of them developed probable or possible AD according to NINDS-ADRDA criteria (McKhann et al., 1984). Normal age-matched controls were recruited from family members of the patients

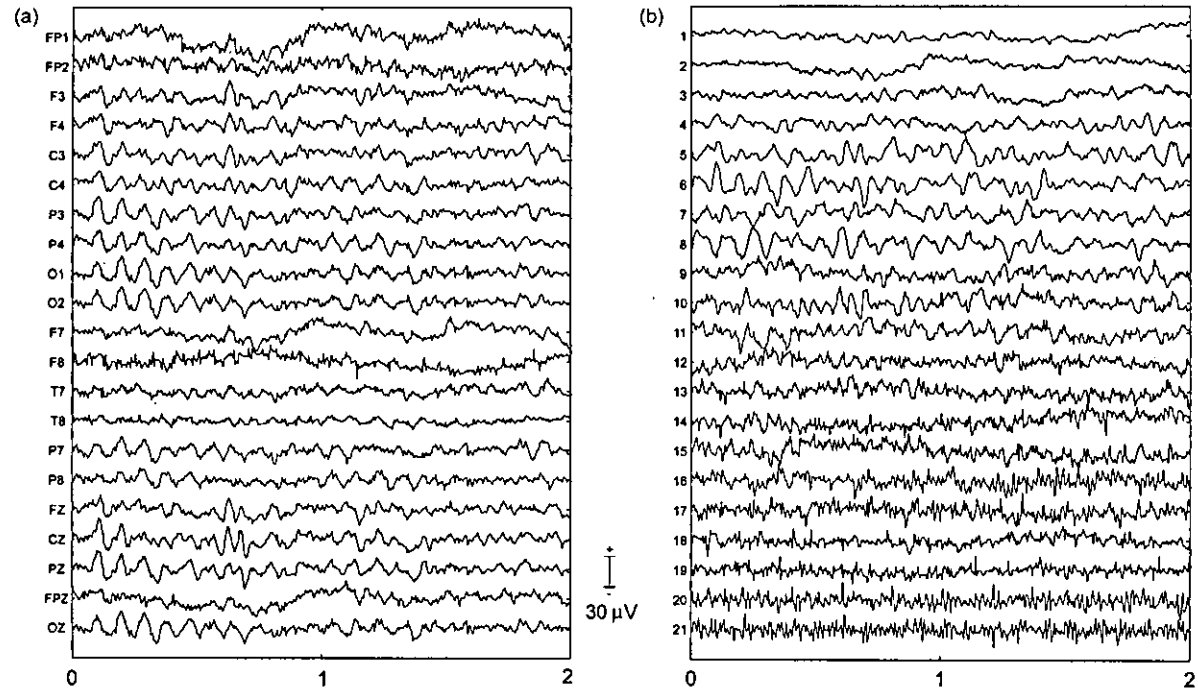

Fig. 1. Example of raw EEG (a) and its components separated with AMUSE algorithm (b) for a patient with MCI who later progressed to AD (MildAD002). AMUSE was applied to 20 s artifact-free interval of EEG, but only 2 s are shown. The scale for the components is arbitrary but linear. Note that the components are automatically ordered according to decreasing linear predictability (increasing complexity).

(mainly spouses) participated in the study as control group. Both patients and controls underwent general medical, neurological, psychiatric, and neuroimaging (SPECT, CT and MRI) investigation for making the diagnosis more precise.

EEG was recorded within 1 month after entering the study from all patients and controls, but only EEG recorded from the patients who progressed to AD ($n=25$; below: MCI group) and age-matched controls ($n=56$) was used for the analysis. No patient or control subject received psychotropic medication at the period when EEG was recorded. Mean MMSE score was 26 ± 1.8 in MCI group and 28.5 ± 1.6 in control group; age 71.9 ± 10.2 and 71.7 ± 8.3, respectively. EEG recording was done in an awake resting state with eyes closed, under vigilance control. Ag/AgCl electrodes (disks of diameter 8 mm) were placed on 21 sites according to 10–20 international system, with the reference electrode on the right ear-lobe. EEG was recorded with Biotop 6R12 (NEC San-ei, Tokyo, Japan) using analog filtering bandpass 0.5–250 Hz and sampling rate 200 Hz.

2.4. EEG data analysis

All computations were done using MATLAB (The MathWorks, Inc.). EEGLAB (Delorme and Makeig, 2004) was used for visual analysis of EEG recordings, and AMUSE algorithm implemented in ICALAB (Cichocki et al., online) was used for BSS processing.

Out of the EEG database described above (from the study of Musha et al., 2002), we selected 25 MCI patients (later progressed to AD) and 47 age-matched controls who had relatively little artifacts. Their EEGs were visually inspected by an experienced EEG researcher and the first continuous artifact-free 20 s interval of each recording was chosen for the analysis. Due to the lack of such interval in some recordings, the number of patients and controls were reduced to 22 and 38, correspondingly. The reason for selecting artifact-free intervals was that most of the artifacts produced amplifier blocking (saturation) due to its low amplitude range, which lead to strongly nonlinear distortion of the signal. AMUSE, as most of BSS methods, assumes a linear model of summation of source signals, and amplifier blocking should be excluded from the data.

Each EEG was decomposed into 21 decorrelated components by BSS algorithm AMUSE (see above). Some of the components (see Results) were selected for back projection, which formed preprocessed ('AMUSE filtered') EEG data. Spectral analysis based on Fast Fourier Transform (Welch method, Hanning 1 s window, 2 s epochs overlapped by 0.5 s) was applied to raw data, to the components and to the projections of selected components. Relative spectral powers were computed by dividing the power in delta (1.5–3.5 Hz), theta (3.5–7.5 Hz), alpha 1 (7.5–9.5 Hz), alpha 2 (9.5–12.5 Hz), beta 1 (12.5–17.5 Hz) and beta 2 (17.5–25 Hz) bands by the power in 1.5–25 Hz band. These values were normalized for better fitting

the normal distribution using the transformation $\ln(x/(1-x))$, where x is the relative spectral power (Gasser et al., 1982). To reduce the number of variables used for classification, we averaged band power values over all 21 channels.

Linear discriminant analysis (LDA) (using publicly available software for both linear classical and robust discriminant analysis, by Croux and Dehon, 2001) was used for discriminating MCI and control groups on the basis of log-transformed relative spectral power in the six frequency bands, averaged over channels. To improve validation of the classification results, discriminant analysis was applied in combination with jack-knifing, a procedure which typically produces lower discrimination rate than, e.g. cross-validation based on using part of a sample for learning and other part for classification, but is statistically more correct and enables increased reproducibility in other samples (Besthorn et al., 1997). Jack-knifing means that each case is classified using individual discriminant function trained with all cases except this one. Results of this procedure was used for computing sensitivity (the number of MCI subjects who were classified as MCI divided by the number of all subjects in MCI group) and specificity (the number of normal subjects who were classified as normal divided by number of all normal subjects).

3. Results

Averaged power spectra of each AMUSE component for patients and control subjects are presented in Fig. 2. As expected, components with lower indices (corresponding to higher linear predictability) had higher relative power at lower frequencies, while components with higher indices had higher relative power at highest frequencies. What is especially important is that the difference between patients and control subjects was clearer in the components with lower indices (i.e. components with highest linear predictability and highest variance of their projections). Thus, in further analysis we used combination of components with lowest indices.

To estimate how many components with highest linear predictability provides optimal classification rate, we applied LDA without jack-knifing (the latter requires much more computation time) to all projected components with indices from 1 to 2, from 1 to 3 and so on. Overall misclassification rate was computed each time by applying obtained discriminant function to the same 60 subjects (22 patients+38 controls). Results are presented in Fig. 3. The best classification was obtained for projection of the first five components (with indices from 1 to 5); however, performance was also high when the number of components

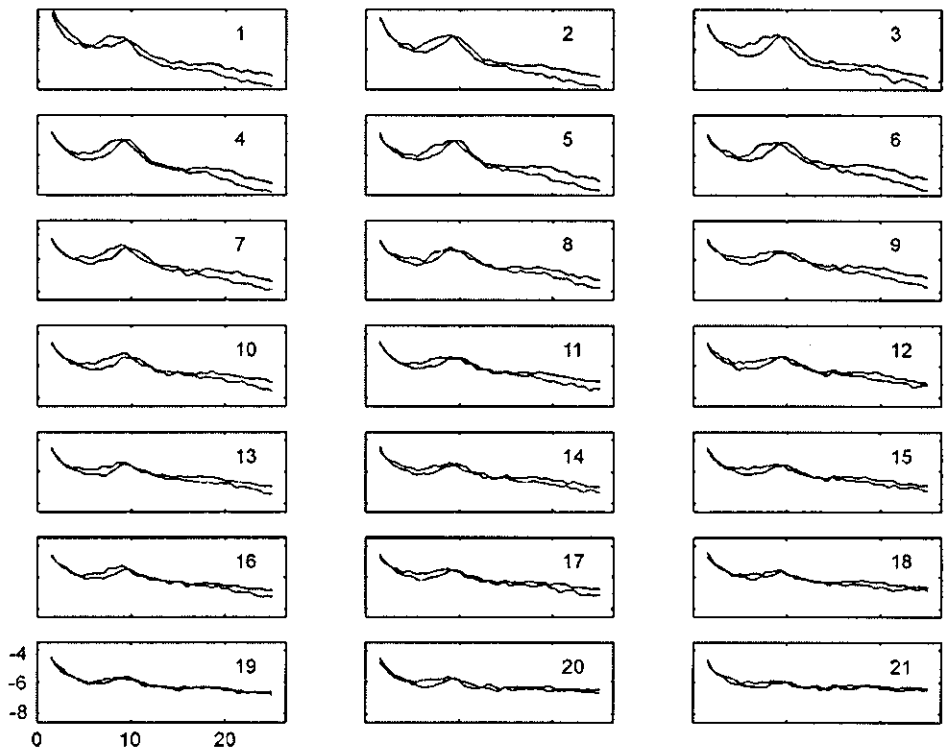

Fig. 2. Averaged power spectra of AMUSE components 1–21. x-axis: frequency, Hz. y-axis: transformed relative spectral power. Relative spectral power was obtained by dividing the absolute values in each frequency bin by total power in the range 1.5–25 Hz. Before averaging, the power values were normalized using transformation $\log(x/(1-x))$ (negative values appear because of this transformation). Red: MCI patients later progressed to AD ($n=22$). Black: control subjects ($n=38$).

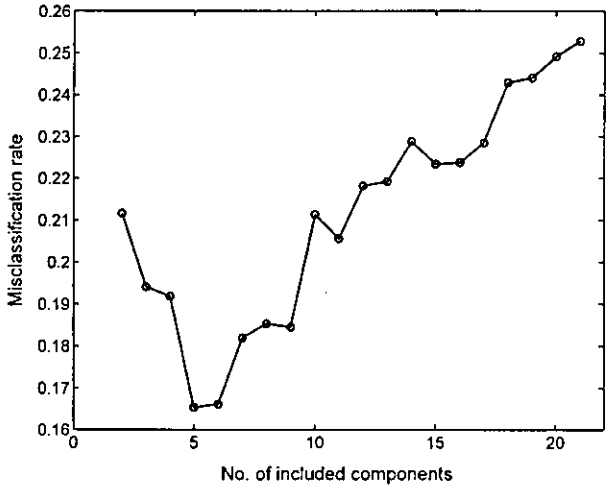

Fig. 3. LDA approximate (computed without cross-validation) misclassification rate for different number of projected components. Only components with highest linear predictability were used, thus, data points correspond to the following combinations of components: 1,2; 1–3; 1–4;..1–20; 1–21.

was in a rather wide range between 3 and 9. Thus, the method appeared to be robust in respect to the number of selected components.

Classification with jack-knifing procedure was applied to projections of several combinations of components, including 1–5 which appeared to be optimal according to Fig. 3. As follows from Table 1, results of classification were better if preprocessing included selection of AMUSE components with lower indices (1–5, 1–7, 1–10), comparing to raw data. When components with higher indices (6–21, 8–21, 11–21) were selected in preprocessing, the results were worse than in the case of raw data. Best results were obtained with components 1–5 and 1–7 (improvement by 14% over the raw data for classification of MCI and by 8% for control subjects), while components 11–21 gave the worst results. More detailed classification results for two combinations of components (1–5 and 1–10) and for the raw data, presented as Relative Operating Characteristic (ROC) curves in Fig. 4, confirm that use of components 1–10 only slightly improved the classification (Fig. 4(a)), while improvement of classification with components 1–5 over raw data was substantial (Fig. 4(b)). Best classification performance after preprocessing using 1–5 components was obtained in the range of approximately 0.6–0.8 for sensitivity and 0.7–0.9 for specificity. Selection of components with high indices was clearly not good for classification: for components 11–21 classification performance was almost at random level (Fig. 4(a)).

Table 1
Number of subjects who were correctly and incorrectly classified by discriminant analysis applied to relative power in six frequency bands after selection and back projection of certain AMUSE components (AMUSE filtering). Results were obtained using jack-knifing

AMUSE components selected in preprocessing	Misclassified		Correctly classified %		
	MCI $n=22$	Controls $n=38$	MCI $n=22$	Controls $n=38$	All $n=60$
No preprocessing	9	9	59	76	70
Components 1–5	**6**	**6**	**73**	**84**	**80**
Components 1–7	**6**	**6**	**73**	**84**	**80**
Components 1–10	6	9	73	76	75
Components 6–21	9	11	59	71	67
Components 8–21	9	11	59	71	67
Components 11–21	**12**	**12**	**45**	**68**	**60**

4. Discussion

With EEG preprocessing proposed in this paper, we obtained 80% rate of correct classification (Table 1) for MCI using only 20 s artifact-free interval of EEG recording from each patient or control subject. While groups of patients and controls were relatively small (22 and 38, correspondingly), it should be noted that the classification performance was estimated using the rigorous jack-knifing cross-validation procedure, which reduce the risk of overstating the results. The jack-knifing procedure was applied only to LDA but not to approximate optimization of the choice of components for back projection. Optimization of the choice of components was made for the whole dataset on the basis of components' spectra and preliminary run of LDA. Nevertheless, Figs. 2 and 3 suggest that the dependence of the difference between patients' and controls' spectra on component index and dependence of LDA results on the number of selected components were systematic; thus, it is unlikely that we simply picked up some random variations in LDA performance dependent on details of preprocessing and that improvement of LDA performance by preprocessing with the same parameters will be not reproducible in other groups of patients and controls.

The procedure of selection of artifact-free EEG intervals used in this study could introduce some bias in absolute values of discrimination results, because it was done by only one expert, and this expert did know to which group each EEG belongs. In fact, the proportion of the EEG recordings which were not analyzed due to the lack of a sufficiently long artifact-free interval was different in the groups of patients (12%) and controls (19%), and this difference was in the direction which can be expected if the criteria for selecting the analyzed interval were more strict for control group. This difference could be a result of random variations, and it should be noted that most of artifacts were easily identifiable (due to low amplifier range, any high amplitude artifact led to amplifier saturation), so it was rather unlikely that the subjective bias could strongly

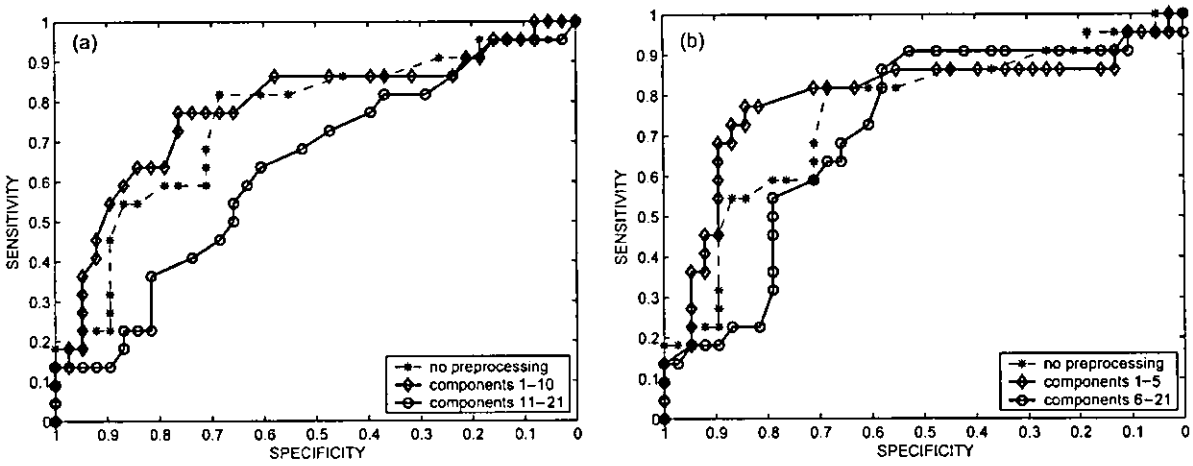

Fig. 4. Relative Operating Characteristic (ROC) curves obtained using jack-knifing for classification of MCI patients later progressed to AD ($n=22$) versus normal controls ($n=38$). LDA was applied to relative power in six EEG frequency bands. Comparison between data without preprocessing and data after selection and back projection of certain AMUSE components (AMUSE filtering). (a) Selection of first 10 components, compared to the rest of components and no preprocessing. (b) Selection of first five components, compared to the rest of components and no preprocessing.

influence the results. However, we cannot guarantee that the use of subjective criteria for selection of artifact free intervals did not affect classification results at all, and it is difficult to predict whether the obtained high values of specificity and sensitivity can be reproduced in other studies. We would like to emphasize, nevertheless, that our main claim is that the proposed preprocessing method increases the performance *relatively* to the level obtained without its use. This tendency could not be altered by subjective bias in search for artifact-free intervals.

We do not discuss here to which physiologically meaningful brain sources AMUSE components can correspond, because they can be a mixture of activity from many physical sources in the brain. This is clearly not critical for improving of EEG classification. The improvement of classification after AMUSE filtering comparing to non-preprocessed EEG data was probably caused by higher difference between patients' and controls' spectra in the selected components than in the non-used (filtered off) components. Spectra computed for AMUSE components separated by BSS algorithm AMUSE (Fig. 2) demonstrate that the difference between patients and controls decreased with the index of component. Interestingly, this effect is visible at the same time in several frequency ranges: in theta range, where patients had an increase of relative power; in alpha range, where shift of the peak to slower frequencies was observed in patients; and in beta range, where relative power was lower for patients. All these differences in spectral power are typically found between AD patients and normal subjects. Spectra of components with the highest indices showed almost no difference between patients and controls, and it was not surprising that the performance of classification based on back projection of only these components was close to random level (Fig. 4(a), components 11–21). Thus, AMUSE components with higher indices can be considered as mainly representing 'noise' which makes difficult, in processing of raw EEG, to detect diagnostically important changes in characteristics of 'signal'. Note that 'signal' and 'noise' here are not labels for signal from brain sources and for artifacts: we refer to the 'signal' only as to diagnostically important (significant) part (subspace) of raw EEG signal, and to 'noise' as to the diagnostically not important part (non-significant subspace). AMUSE filtering, i.e. extraction of part of EEG reach with 'signal' by using only 'best' (here, most useful for diagnosis) components for back projection, naturally leads to the improvement of 'signal-to-noise ratio' and, as a result, to the improvement of EEG classification.

A BSS-based approach to improvement of signal-to-noise ratio in MEG signal by defining and removing noise subspace was already developed (Kawakatsu, 2003). More simple and already rather widely used technique is removing EEG and MEG artifact-related components with BSS using visual or automatic identification of such components one by one after decomposition (e.g. Jung et al., 2000). However, since in many kinds of EEG and MEG studies the goal is to extract the brain signal in possibly less distorted form, the existing techniques are limited to remove only such part of raw signal, which contain no or almost no components of brain origin but rather external artifacts and noise. In EEG classification tasks, such as diagnosis or Brain-Computer Interface (BCI), preserving the original signal is less important, noise can be defined not only as artifacts but also as any part of the signal which do not contribute to the difference between the classes of EEG which should be differentiated, and larger subspace with high percentage of such 'noise' can be removed. The existing techniques can only identify, by some a priori known characteristics, noise components (Barbati et al., 2004; Jung et al., 2000; Kawakatsu, 2003)

and some very specific diagnostically important components (epileptic spike separation: e.g. Kobayashi et al., 2002). Xu et al. (2004) recently suggested using a subspace approach for differentiating between task-related EEG patterns in BCI. They selected several ICA components related to P300 according to the a priori knowledge of P300 spatio-temporal pattern and reconstructed a clear P300 peak using back projection of these components. Like in the case of epileptic spikes, the components in this case were easily identifiable.

In a general case, however, significant and non-significant components are not easily identifiable. The task becomes especially challenging if EEG components from different subjects should be compared, because the sets of components produced by BSS in different subjects usually differ dramatically. In our approach, we rank components using some empirical rule, such as their linear predictability, and select those where difference between the pathological and normal EEG is most differentiated. This made possible to achieve substantial improvement in the discrimination between MCI patients who later progressed to AD and normal age-matched controls. To our best knowledge, no study till now investigated the application of BSS/ICA methods as preprocessing tools with possible application for AD diagnosis.

Dividing of components into two groups (or subspaces) as below or above some component's index (in the case of ranking) or using a threshold for some index computed for each component is not the only way. One may try to divide the sets of components at more than one level and, e.g. remove not only components with highest indices but also with the lowest indices. As one may suppose from Fig. 1(b) (example of individual data), the first two components could represent, to rather high extent, artifacts (roving eye movements). Fig. 2, however, shows that components #1 and #2 substantially differed between groups. We made an attempt to exclude 1 or 2 first components from the analysis and this, in fact, led to slightly lower discrimination results. However, it is possible that for other data (for example, including high amplitude low frequency artifacts) or other processing techniques dividing the set of components on more than one level could be beneficial.

Not only spectral but also other EEG features, such as measures of synchronization between channels, can be investigated for the possibility of improving contrast between pathological and normal data using the presented approach. Several studies indicated that synchronization between different brain areas is sensitive to AD. Such results were obtained for quite different techniques, including coherence (e.g. Adler et al., 2003; Jelic et al., 1996; Locatelli et al., 1998; Wada et al., 1998), mutual information (Jeong et al., 2001) and synchronization likelihood (a new measure combining estimation of linear and nonlinear coupling) (Stam et al., 2003). One may hypothesize that EEG components can be divided into two parts, one of which represents signal subspace with lower (or stronger) synchronization among some cortical areas in AD relative to normal EEG, and another one represents signal subspace which synchronization characteristics are not related to the disease. In this case, the general approach described in this paper also could appear to be useful. One may probably try to apply it also in the case of using nonlinear measures (see review in Jeong, 2004) or in combination with other advanced approaches.

There is obviously room for improvement and extension of the proposed method both in ranking and selection of optimal (significant) components, apparatus and post-processing to perform classification task. Especially, we can apply a wide variety of BSS methods, i.e. instead of the applied and investigated second order statistics spatio-temporal decorrelation, we can exploit other new types of BSS algorithms, such as higher order statistic ICA, sparse component analysis or smooth component analysis with a suitably ordered and ranked components. Furthermore, instead of standard LDA we can use more sensitive and robust methods, such as neural networks or support vector machine (SVM) classifiers. Classification can be probably strongly improved by supplementing the set of spectral power values which we used with much different indices, such as alpha dipolarity, a new index depending on prevalence local vs. distributed sources of EEG alpha activity, which was shown to be very sensitive to AD-related cortical impairment (Musha et al., 2002). Additional attractive but still open issue is that using the proposed approach, we can not only detect but also measure in consistent way the progression of AD and influence of medications. The proposed method can also be potentially useful and effective tool for differential diagnosis of AD from other types of dementia, and possibly for diagnosis of other diseases. Other areas of EEG analysis can be also possible field for the application of our preprocessing technique. For these purposes, more studies would be needed to asses of the impact of the proposed enhancement/filtering procedures on the EEG signal of interest.

References

Adler G, Brassen S, Jajcevic A. EEG coherence in Alzheimer's dementia. J Neural Transm 2003;110(9):1051–8.

Barbati G, Porcaro C, Zappasodi F, Rossini PM, Tecchio F. Optimization of an independent component analysis approach for artifact identification and removal in magnetoencephalographic signals. Clin Neurophysiol 2004;115(5):1220–32.

Belouchrani A, Abed-Meraim K, Cardoso JF, Moulines E. A blind source separation technique using second order statistics. IEEE Trans Signal Process 1997;45(2):434–44.

Besthorn C, Zerfass R, Geiger-Kabisch C, Sattel H, Daniel S, Schreiter-Gasser U, et al. Discrimination of Alzheimer's disease and normal aging by EEG data. Electroencephalogr Clin Neurophysiol 1997; 103(2):241–8.

Blennow K, Hampel H. CSF markers for incipient Alzheimer's disease. Lancet Neurol 2003;2(10):605–13.

Cichocki A, Amari S. Adaptive blind signal and image processing: learning algorithms and applications. New York, NY: Wiley; 2003.

Cichocki A, Amari S, Siwek K, Tanaka T, et al. ICALAB toolboxes. [Available online at http://www.bsp.brain.riken.jp/ICALAB]

Croux C, Dehon C. Software package for robust discriminant analysis; 2001. [http://www.econ.kuleuven.ac.be/public/NDBAE06/software/DA/matlab.htm]

DeKosky ST, Marek K. Looking backward to move forward: early detection of neurodegenerative disorders. Science 2003;302(5646): 830–4.

Delorme A, Makeig S. EEGLAB: an open source toolbox for analysis of single-trial EEG dynamics including independent component analysis. J Neurosci Methods 2004;134(1):9–21.

Gasser T, Bacher P, Mocks J. Transformations towards the normal distribution of broad band spectral parameters of the EEG. Electroencephalogr Clin Neurophysiol 1982;53(1):119–24.

Goncharova II, McFarland DJ, Vaughan TM, Wolpaw JR. EMG contamination of EEG: spectral and topographical characteristics. Clin Neurophysiol 2003;114(9):1580–93.

Hara J, Shankle WR, Musha T. Cortical atrophy in Alzheimer's disease unmasks electrically silent sulci and lowers EEG dipolarity. IEEE Trans Biomed Eng 1999;46(8):905–10.

Hodges JR. Cognitive assessment for clinicians. Oxford: Oxford Medical Publications; 1993 p. 197–228.

Huang C, Wahlund L, Dierks T, Julin P, Winblad B, Jelic V. Discrimination of Alzheimer's disease and mild cognitive impairment by equivalent EEG sources: a cross-sectional and longitudinal study. Clin Neurophysiol 2000;111(11):1961–7.

Jelic V, Shigeta M, Julin P, Almkvist O, Winblad B, Wahlund LO. Quantitative electroencephalography power and coherence in Alzheimer's disease and mild cognitive impairment. Dementia 1996;7(6): 314–23.

Jeong J. EEG dynamics in patients with Alzheimer's disease. Clin Neurophysiol 2004;115(7):1490–505.

Jeong J, Gore JC, Peterson BS. Mutual information analysis of the EEG in patients with Alzheimer's disease. Clin Neurophysiol 2001;112(5): 827–35.

Joyce CA, Gorodnitsky IF, Kutas M. Automatic removal of eye movement and blink artifacts from EEG data using blind component separation. Psychophysiology 2004;41(2):313–25.

Jung TP, Makeig S, Westerfield M, Townsend J, Courchesne E, Sejnowski TJ. Removal of eye activity artifacts from visual event-related potentials in normal and clinical subjects. Clin Neurophysiol 2000;111(10):1745–58.

Kawakatsu M. Application of ICA to MEG noise reduction. Fourth international symposium on independent component analysis and blind signal separation (ICA2003), Nara, Japan; April 1–4, 2003, p. 535–41.

Kobayashi K, Akiyama T, Nakahori T, Yoshinaga H, Gotman J. Systematic source estimation of spikes by a combination of independent component analysis and RAP-MUSIC. II: preliminary clinical application. Clin Neurophysiol 2002;113(5):725–34.

Locatelli T, Cursi M, Liberati D, Franceschi M, Comi G. EEG coherence in Alzheimer's disease. Electroencephalogr Clin Neurophysiol 1998; 106(3):229–37.

McKhann G, Drachman D, Folstein M, Katzman R, Price D, Stadlan EM. Clinical diagnosis of Alzheimer's disease: report of the NINCDS-ADRDA Work Group under the auspices of Department of Health and Human Services Task Force on Alzheimer's Disease. Neurology 1984; 34(7):939–44.

Musha T, Asada T, Yamashita F, Kinoshita T, Chen Z, Matsuda H, et al. A new EEG method for estimating cortical neuronal impairment that is sensitive to early stage Alzheimer's disease. Clin Neurophysiol 2002; 113(7):1052–8.

Petersen RC, editor. Mild cognitive impairment: aging to Alzheimer's Disease. New York: Oxford University Press. 2003.

Pritchard WS, Duke DW, Coburn KL, Moore NC, Tucker KA, Jann MW, et al. EEG-based, neural-net predictive classification of Alzheimer's disease versus control subjects is augmented by non-linear EEG measures. Electroencephalogr Clin Neurophysiol 1994; 91(2):118–30.

Rapoport SI. Functional brain imaging to identify affected subjects genetically at risk for Alzheimer's disease. Proc Natl Acad Sci USA 2000;97(11):5696–8.

Stam CJ, van der Made Y, Pijnenburg YA, Scheltens P. EEG synchronization in mild cognitive impairment and Alzheimer's disease. Acta Neurol Scand 2003;108(2):90–6.

Szupiluk R, Cichocki A. Blind signal separation using second order statistics. Proceedings of SPETO; 2001, p. 485–8.

Tang AC, Pearlmutter BA, Malaszenko NA, Phung DB. Independent components of magnetoencephalography: single-trial response onset time estimation. NeuroImage 2002;17:1773–89.

Tong L, Soon V, Huang YF, Liu R. Indeterminacy and identifiability of blind identification. IEEE Trans CAS 1991;38:499–509.

Tong L, Inouye Y, Liu R. Waveform-preserving blind estimation of multiple independent sources. IEEE Trans Signal Process 1993;41(7): 2461–70.

Vorobyov S, Cichocki A. Blind noise reduction for multisensory signals using ICA and subspace filtering, with application to EEG analysis. Biol Cybern 2002;86(4):293–303.

Wada Y, Nanbu Y, Koshino Y, Yamaguchi N, Hashimoto T. Reduced interhemispheric EEG coherence in Alzheimer disease: analysis during rest and photic stimulation. Alzheimer Dis Assoc Disord 1998;12(3): 175–81.

Wagner AD. Early detection of Alzheimer's disease: an fMRI marker for people at risk. Nat Neurosci 2000;3(10):973–4.

Wechsler D. Wechsler memory scale: revised manual. San Antonio, TX: Psychological Corp.; 1987.

Xu N, Gao X, Hong B, Miao X, Gao S, Yang F. BCI Competition 2003—Data set IIb: enhancing P300 wave detection using ICA-based subspace projections for BCI applications. IEEE Trans Biomed Eng 2004;51(6): 1067–72.

Original article

Nuclear Medicine Communications

Gender difference in brain perfusion ^{99m}Tc-ECD SPECT in aged healthy volunteers after correction for partial volume effects

Zhi-Jie Li[a,c], Hiroshi Matsuda[a], Takashi Asada[b], Takashi Ohnishi[a], Hidekazu Kanetaka[a], Etsuko Imabayashi[a] and Fumiko Tanaka[a]

Background Previous reports have yielded controversial results concerning gender differences in regional cerebral blood flow (rCBF). To elucidate this issue, we compared ^{99m}Tc ethyl cysteinate dimer single photon emission computed tomography (SPECT) images for brain perfusion between aged-matched healthy men and women after correction for partial volume effects (PVEs).

Methods Brain perfusion SPECT in the resting state was performed on 40 healthy, right-handed subjects, 20 men and 20 women, with an age range of 58–86 years, who did not differ sociodemographically. PVE correction was performed using grey matter volume measured by magnetic resonance imaging. Statistical parametric mapping was used for the analysis of the adjusted rCBF images of relative flow distribution.

Results The PVE correction revealed that women had higher rCBF in left inferior frontal gyrus, bilateral middle temporal gyri, and left superior temporal gyrus. Men had higher rCBF in left superior frontal gyrus, right medial frontal gyrus, right superior parietal lobule, right postcentral gyrus, right cerebellum, right middle frontal gyrus, right fusiform gyrus, and right precuneus.

Conclusion Significant gender differences in rCBF existed in these healthy volunteers. The PVE correction of SPECT images revealed gender differences that were consistent with the universal findings of better performance on verbal tasks in women and on visuospatial tasks in men. *Nucl Med Commun* 25:999–1005 © 2004 Lippincott Williams & Wilkins.

Nuclear Medicine Communications 2004, 25:999–1005

Keywords: single photon emission computed tomography, ^{99m}Tc ethyl cysteinate dimer, regional cerebral blood flow, gender

[a]Department of Radiology, National Center Hospital for Mental, Nervous, and Muscular Disorders, National Center of Neurology and Psychiatry, Tokyo, [b]Department of Neuropsychiatry, Institute of Clinical Medicine, University of Tsukuba, Ibaraki and [c]Department of Nuclear Medicine, The Second Clinical Hospital of China Medical University, Shen-Yang City, China.

Correspondence to Dr Hiroshi Matsuda, Department of Nuclear Medicine, Saitama Medical School Hospital, 38 Morohongo Moroyama-machi, Iruma-gun, Saitama, 350-0495, Japan.
Tel: +81 49 276 1302; fax: +81 49 276 1301
e-mail: matsudah@saitama-med.ac.jp

Received 10 October 2003 Revised 18 March 2004
Accepted 25 March 2004

Introduction

Gender differences in behaviours such as cognitive and emotional processing are increasingly recognized. Such differences are considered to have biological substrates. Neuropsychological measures have demonstrated gender differences [1–3]. Functional neuroimaging techniques such as positron emission tomography (PET) and single photon emission computed tomography (SPECT) have also been used to observe the gender differences in regional cerebral blood flow (rCBF) or regional cerebral metabolic rate for glucose (rCMRglc) quantitatively or semiquantitatively [3–13], but at present the findings are controversial. Although some studies indicated that gender differences exist in both rCBF and rCMRglc, the regions focused on in the various studies were not entirely consistent. Nevertheless, others reported no gender based differences [5,6]. Many factors are likely to have contributed to these discrepancies, including differences in the normal subjects selected, tracers and scanners, and methods of analysis. One possible explanation is an interaction between a subject's age and gender, because studies reported that differences between the sexes occur in younger cohorts only and become less prominent in later years [14–16]. Further, even when gender differences are observed, it is still unclear whether the differences in PET or SPECT imaging between women and men reflect true gender differences of rCBF or rCMRglc. Due to the limited spatial resolution of PET or SPECT, the accurate measurement of tracer concentration in brain structures depends on several physical limitations, particularly the relation between object size and scanner spatial resolution. This relation, known as the partial volume effect (PVE), biases the measured concentration in small structures by diminishing the true concentration. The PVE causes a volume averaging effect between the tissue elements of grey matter, white matter, and cerebrospinal fluid in a region of the brain. Since the results of magnetic resonance imaging (MRI)

studies have demonstrated gender related differences in brain morphology [17,18], PVE may exert an influence on PET and SPECT results. Van Laere and Dierckx [13] considered the regional structure of the brain tissue when they studied gender differences, but used an indirect method, comparing the grey matter volume and brain perfusion. No voxel based PVE correction was done in the gender difference study with PET or SPECT. Recently, the high-resolution anatomical detail available with MRI techniques has led to the development of magnetic resonance based methods to correct PET or SPECT data for PVE [19–24]. In the present research our aim was to investigate the gender difference in aged healthy volunteers using brain perfusion SPECT imaging and to determine which brain structures show a greater influence of PVE correction.

Methods

Study population

A sample of 40 right handed healthy adults, 20 women and 20 men, with an age range of 58–86 years was recruited from spouses of patients with Alzheimer's disease who were referred to the memory clinic of our hospital. These healthy aged subjects were known not to have cognitive changes during the follow-up period of more than 2 years since these spouses were attendant for the patients. They had no neurological or psychiatric disorders, including alcoholism, substance abuse, atypical headache, head trauma with loss of consciousness, or asymptomatic cerebral infarction detected by T2 weighted MRI. Women and men did not differ socio-demographically; age (mean ± SD), women 68.4 ± 7.4, men 72.4 ± 7.5; education, women 13.0 ± 2.2, men 13.8 ± 2.0; verbal IQ [25], women 117.9 ± 9.1, men 121.2 ± 6.9; performance IQ, women 114.3 ± 9.3, men 110.7 ± 9.3; total IQ, women 117.4 ± 8.1, men 117.6 ± 6.8; two-sample t-test, all two-tailed $P > 0.3$. There were no significant differences between men and women in the Mini-Mental State Examination [26]: women 29.3 ± 0.9, men 28.6 ± 1.4, and scores of Wechsler memory scales (revised) [27], either. The ethics committee of our centre approved this study for healthy volunteers, all of whom gave their informed consent to participate.

SPECT study and PVE correction

Before SPECT was performed, an intravenous line was established in all subjects. They were injected while lying down in the supine position with eyes closed in a dimly lit, quiet room. Each received a 600 MBq intravenous injection of ^{99m}Tc ethyl cysteinate dimer (^{99m}Tc-ECD). Ten minutes after the injection of ^{99m}Tc-ECD, brain SPECT was performed using a triple-head SPECT system (Multispect 3; Siemens Medical Systems Inc., Hoffman Estates, IL) equipped with high-resolution fanbeam collimators. For each camera, projection data were obtained in a 128 × 128 format for 24 angles of 120° at 50 s per angle. A Shepp and Logan Hanning filter was used as a filtered back-projection method for SPECT image reconstruction at 0.7 cycle/cm. Attenuation correction was performed using Chang's method with an optimized effective attenuation coefficient of 0.09 cm^{-1}.

Correction for PVE was performed for atrophy correction in SPECT images using three dimensional volumetric T1 weighted magnetic resonance (MR) images (a 1.0 T system; Magnetom Impact Expert, Siemens, Erlagen, Germany) as described in previous studies [23,24]. A three-dimensional volumetric acquisition of a T1 weighted gradient-echo sequence produced a gapless series of thin sagittal sections using a magnetization preparation rapid acquisition gradient-echo sequence (TE/TR, 4.4/11.4 ms; flip angle, 15°; acquisition matrix, 256 × 256; slice thickness, 1.23 mm). The MR images acquired were reformatted to gapless 2 mm thick transaxial images. Then MR images were converted to the same isometric matrix size as that for SPECT images. Then Statistical Parametric Mapping 99 (SPM99, www.fil.ion.bpmf.ac.uk/spm/) segmented these isometric MR images into grey matter, white matter, cerebrospinal fluid, and other compartments. The segmentation procedure involves calculating, for each voxel, a Bayesian probability of belonging to each tissue class based on *a priori* MRI information with inhomogeneity correction for the magnetic field. The Automated Image Registration (AIR) software (www.loni.ucla.edu/NCRR/Software/AIR.htm) was used to align the SPECT to the MRI scans of each subject using a six-parameter rigid-body transformation. Prior to co-registration of SPECT and MRI, the outer scalp was removed from MRI by applying a binary mask for the whole brain mentioned later to the MRI. A three-dimensional convolution with the point spread function of the SPECT device (assumed to be a simple three dimensional Gaussian with full width at half maximum (FWHM) of 9.0 × 9.0 × 9.0 mm), was performed to obtain coefficients of dispersion for each voxel. This procedure of identification of spatial resolution between grey matter SPECT and MR images makes it possible to correct PVE by division of these two images in the final procedure. These convoluted grey matter and white matter images were normalized to have a maximum count of 1.0 as 32 bit real values. A binary volume image was created from this convoluted grey matter image with the threshold set to 35% of the maximum value as a mask image for grey matter. A mask image for the whole brain was created from this mask image for grey matter by filling the interior holes in the brain. Then white matter SPECT images were simulated from these normalized white matter MR images with convolution as follows. The maximum count of 1.0 for the normalized white matter MR image was replaced by the maximum SPECT count in the white matter. To get the maximum count for the white matter of SPECT, a region of interest (ROI) was automatically determined by setting the threshold to

above 95% of the maximum count density of the white matter MR images. The grey matter SPECT images were obtained by subtraction of these white matter SPECT images from the original SPECT images co-registered to MRI. Last, the grey matter SPECT image was divided by the normalized grey matter MR image with equivalent spatial resolution to SPECT on a voxel-by-voxel basis. The mask image for grey matter was applied to this divided image. In the present study, a fully automated program for the PVE correction was developed using C + + language.

Image formatting and analysis

All subsequent image manipulation and data analysis were performed on a personal computer with an operating system of Windows XP. Grey matter SPECT images before and after atrophy correction and convoluted grey matter images segmented from MRI were spatially normalized in SPM99 to a standardized stereotactic space based on the Talairach and Tournoux atlas [28], using 12-parameter linear affine normalization and further 12 non-linear iteration algorithms with an original template for ^{99m}Tc-ECD [29] and with a template for *a priori* grey matter of SPM99 respectively. Then, images were smoothed using a 12 mm FWHM isotropic Gaussian kernel. The initial parameters of the image matrix were $128 \times 128 \times n$, where n is the number of slices covering the whole brain. The final image format is 16-bit, with a matrix size of $79 \times 95 \times 68$ and a voxel size $2 \times 2 \times 2$ mm.

Data sets were handled with SPM99. Women and men were compared using the 'compare population one scan/subject' routine, which carries out a fixed effects simple t-test for each voxel. The 'proportional scaling' routine was used to control for individual variation in global ^{99m}Tc-ECD uptake; these data will be referred to as 'adjusted rCBF.' The grey matter threshold was set at 80% of whole brain mean. Gender differences in grey matter concentration were also examined using voxel based morphometry as described in a previous study [30]. The resulting set of values for each contrast constituted a statistical parametric map of the t statistic SPM{t}. The SPM{t} maps were then transformed to the units of normal distribution (SPM{Z}), and height threshold was set to $P < 0.005$ with cluster extent $K > 100$ voxels. Anatomical localization was according to Talairach coordinates, obtained from Brett's transformations (www.mrc-cbu.cam.ac.uk/Imaging/mnispace.html).

Results

Spatially normalized SPECT images for average in 20 healthy men and 20 healthy women were shown before and after PVE correction in Fig. 1. The PVE correction made the rCBF distribution more homogenous than the original distribution.

Before PVE correction, women showed higher perfusion in left superior temporal gyrus and left supramarginal gyrus than men. On the other hand, men showed higher perfusion in right medial frontal gyrus, bilateral middle frontal gyri, right fusiform gyrus, and right cerebellum than women (Fig. 2, Table 1).

After PVE correction, women showed higher perfusion in left inferior frontal gyrus, bilateral middle temporal gyri, and left superior temporal gyrus than men. Meanwhile, men showed higher perfusion in left superior frontal gyrus, right medial frontal gyrus, right superior parietal lobule, right postcentral gyrus, right cerebellum, right middle frontal gyrus, right fusiform gyrus, and right precuneus than women (Fig. 2, Table 1).

Women showed larger grey matter volume in left superior temporal gyrus than men (Fig. 3, Table 2). Meanwhile men showed larger grey matter volume in bilataral superior frontal gyri, bilateral medial frontal gyri, and left precentral gyrus than women (Fig. 3, Table 2).

Discussion

Although several investigators have examined gender differences in healthy volunteers using PET or SPECT, the findings of these studies have been inconsistent and controversial. In the present SPECT study we investigated gender differences in the relative distribution of brain perfusion and moreover examined the modifications that occur after correction for PVE. Totally significant gender differences in rCBF were noted in the present study, with PVE correction found to mostly influence frontal and parietal lobes.

A consistent finding in gender differences in behaviours is that women perform better than men on some verbal tasks [2]. Women tend to perform better on verbal learning and recall tasks [3]. The present correction for PVE compensated for the lower spatial resolution of SPECT compared with PET and possibly increased sensitivity in detecting rCBF differences between women and men. Although there is no reason why a region that performs differently under activation should have different perfusion at rest, the present results after PVE correction were more in line with a verbal fluency test which involved frontal areas than were results before PVE correction. Audenaert *et al.* [31] found that the activation paradigm of verbal fluency using SPECT caused a rCBF increase in left inferior frontal gyrus.

Moreover, PVE correction of SPECT images led to greater similarity of the present results to previously reported results using PET in which women showed higher resting rCBF in bilateral mid-temporal regions [7]. The finding of higher rCBF in women than in men disappeared after PVE correction in a supero-posterior